Plasmonic triple-wavelength demultiplexing structure based on metal-insulator-metal waveguides side-coupled with nanoring cavities

Xu Siyu, Zhang Zhaojian, He Xin, Han Yunxin, Zhang Jingjing, Huang Jie, Chen Dingbo, Yang Junbo*

(College of Liberal Arts and Sciences, National University of Defense Technology, Changsha 410073, China)

Abstract: A plasmonic triple-wavelength demultiplexing structure based on metal-insulator-metal waveguides side-coupled with nanoring cavities was proposd by studying theoretically and numerically. The structure consisted of three output channels, each of which was sandwiched by two nanoring cavities. By changing the filling medium of the ring and the relative position of the inner and outer circle, the reflection and transmission spectrum of each channel could be dynamically tunable. Finally, according to the reflection and transmission characteristics of three channels, the demultiplex at three telecommunication wavelengths 1 310 nm, 1 490 nm and 1 550 nm with excellent performance was studied. Temporal coupled-mode (CMT) theory and finite-difference time-domain (FDTD) method are applied to simulation and analysis, and this work can find potential applications for on-chip integrated all-optical circuits.

Key words: plasmonic; demultiplexing; finite-difference time-domain; metal-insulator-metal; nanoring cavity

CLC number: TN256 **Document code:** A **DOI:** 10.3788/IRLA201948.0221001

基于金属-绝缘体-金属波导耦合纳米腔的等离子体三波分复用结构

徐思宇,张兆健,何 新,韩云鑫,张晶晶,黄 杰,陈丁博,杨俊波*

(国防科技大学 文理学院,湖南 长沙 410073)

摘 要: 从理论上和数值上研究了一种基于金属-绝缘体-金属波导耦合纳米腔的等离子体三波分复用结构。该结构由三个输出通道组成,每个通道由两个纳米腔分布于直波导两侧。通过改变环的几何参数、填充介质和内圆和外圆的相对位置,可以动态地调节每个通道的反射和透射光谱。最后,根据三个通道的反射和透射特性,研究了在三个通信波长 1 310、1 490 和 1 550 nm 处实现的解复用,并具有优良的性能。将时域耦合模理论和时域有限差分法(FDTD)结合起来进行仿真和分析,为芯片集成全光电路的应用提供了可能。

关键词: 等离子体; 解复用; 时域有限差分法; 金属绝缘体金属; 纳米腔

收稿日期: 2018-09-07; **修订日期:** 2018-10-12

基金项目: 国家自然科学基金(6090700361671455);NUTD(JC13-02-13,ZK17-13-01);湖南省自然科学基金(13JJ3001);新世纪大学优秀人才计划(NCET-12-0142)

作者简介: 徐思宇(1994-),男,硕士生,主要从事微纳米光电子技术方面的研究。Email: 13149600390@163.com

导师简介: 杨俊波(1974-),男,副教授,博士,主要从事微纳米光电子技术方面的研究。Email: yangjunbo@nudt.edu.cn

0 Introduction

Surface plasmon polaritons(SPPs), are surface electromagnetic waves occurring due to the coupling between incident radiation and collective electron oscillations at the metal –dielectric interfaces. SPPs have been widely studied during the past decades because of overcoming the conventional diffraction limits and manipulating light on deep subwavelength scales at the same time[1].

A variety of SPP–based waveguide structures have been proposed, such as metallic strips and nanowires, channel plasmon waveguides, dielectric–loaded SPPs, and metal–insulator–metal (MIM) structures. Among those structures, the MIM waveguide supports surface–plasmon modes and strongly confines the incident light in the dielectric region with acceptable propagation length and zero–bend loss[2].

Recently, various devices based on SPPs such as filters, demodulators, switches, and splitters are simulated numerically and demonstrated experimentally. To guide the plasmonic waves for various applications, MIM waveguides are utilized. The MIM structure which strongly confines the incident light in the insulator region is promising for the design of compact all–optical devices owing to a relatively easy fabrication. In the past few years, some devices based on the MIM waveguide have been proposed and studied numerically, such as plasmonic sensors, plasmonic switches, plasmonic splitters, plasmonic filters, and plasmonic demultiplexers[3].

The plasmonic wavelength demultiplexers with ultra–small scale will play an important role in highly integrated on–chip optical communication systems. The rectangular cavities have been extensively utilized to realize various wavelength demultiplexing structures, including the side–coupled slot cavities, nanocapillary resonators, and Fabry–Perot resonators[4]. Compared with the rectangular cavity, the disk–shaped cavity has only one geometrical parameter to control, i.e., radius, which has been investigated to design a multichannel wavelength demultiplexer.

In this paper, we numerically propose a plasmonic triple–wavelength demultiplexing structure based on metal–insulator–metal waveguides side–coupled with nanoring cavities. Each output channel consists of two side–coupled cavities and acts as a dual band–stop plasmonic filter. The transmission characteristics are analyzed by using the theoretical model and finite–difference time–domain (FDTD) simulation. The operating principle and performance of the structure are discussed. The demultiplexed wavelength at each channel can be effectively manipulated by adjusting the geometrical parameters. By selecting the appropriate geometric parameters, the wavelength demultiplexing at three telecommunication wavelengths 1 310 nm, 1 490 nm and 1 550 nm can be realized. This work can find potential applications for on–chip integrated all–optical circuits.

1 Operation principle of the dual band–stop filter structure

Figure 1 shows the plasmonic band–stop filter structure, which is composed of an MIM waveguide and a side–coupled nanoring cavity. Since the width of the MIM waveguide is much

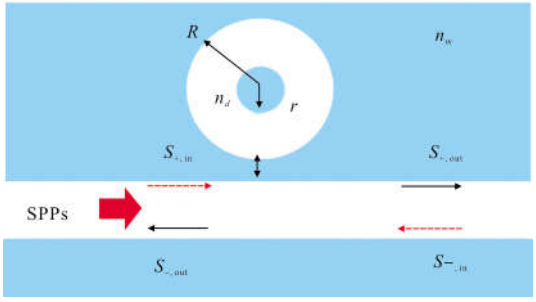

Fig.1 Schematic of a plasmonic band–stop filter structure

smaller than the incident wavelength, only the fundamental TM mode could be excited. The complex propagation constant β_{spp} of the MIM waveguide can be obtained from the following dispersion equations[5].

$$\varepsilon_d k_m+\varepsilon_m k_d \tanh\left(\frac{\omega k_d}{2}\right)=0 \tag{1}$$

$$k_{d,m}=\sqrt{\beta_{spp}^2-\varepsilon_{d,m}k_0^2} \tag{2}$$

where ε_m and ε_d are the dielectric constants of the metal and dielectric core, respectively, $k_0=2\pi/\lambda$ is the propagation constant in vacuum, and $k_{d,m}$ are the propagation constants in the dielectric and the metal regions, respectively. Throughout the paper, the metal is assumed as silver, whose wavelength dependent permittivity with the metal loss included is taken from the literature [6]. The dielectric material is assumed to be Al_2O_3(n_d=1.7).

The operation principle for band-stop filtering can be understood by analyzing the propagation behavior of SPPs in the proposed structure. The structure has mirror symmetry with respect to the reference plane. As the SPPs propagate in the MIM waveguide, the energy can be coupled into the nanoring resonator. The single nanoring transmission spectrum will exhibit a dip at the resonance wavelength due to the destructive interference between the incident field and the escaped field from the resonator. The transmission characteristics of the structure could be investigated by the temporal coupled-mode theory [7]. As shown in Fig.1, the amplitudes of the incoming and outgoing light are denoted by $S_{d,\text{in}}$ and $S_{d,\text{out}}$, and are normalized to the energy carried by the waveguide mode. The subscript d indicates ±, representing the forward -and backward - propagating SPPs. For simplicity, the light propagation and coupling losses are neglected in the temporal coupled-mode analysis[8]. For the harmonic time dependence of $\exp(j\omega t)$, the time evolution of the normalized amplitude a of the cavity in steady state can be described as:

$$\frac{da}{dt}=(-j\omega_r-\kappa_o-\omega_e)a+\exp(j\theta)\sqrt{\kappa_e}S_{+,\text{in}}+\exp(j\theta)\sqrt{\kappa_e}S_{-,\text{in}} \tag{3}$$

where ω_r is the resonance frequency of the nanoring cavity, κ_o is the decay rate of the field due to internal loss in the cavity, and κ_e is the decay rate due to the energy coupled into the waveguide. θ is the phase of coupling coefficients between the cavity and the MIM waveguide. The relationships between the amplitude of nanoring cavity and the incoming/outgoing light in the MIM waveguide are described as:

$$S_{+,\text{out}}=S_{+,\text{in}}-\exp(-j\theta)\sqrt{\kappa_e}a \tag{4}$$

$$S_{-,\text{out}}=S_{-,\text{in}}-\exp(-j\theta)\sqrt{\kappa_e}a \tag{5}$$

The waveguide mode field at a frequency ω is launched from the input port of the MIM waveguide, i.e.,$S_{-,\text{in}}=0$ and $da/dt=j\omega a$. Based on the above equations, the transmission T and reflection R of the filter can be derived as:

$$T=\left|\frac{S_{+,\text{out}}}{S_{+,\text{in}}}\right|^2=\frac{\kappa_o^2+(\omega-\omega_r)^2}{(\kappa_o+\kappa_e)^2+(\omega-\omega_r)^2} \tag{6}$$

$$R=\left|\frac{S_{-,\text{out}}}{S_{-,\text{in}}}\right|^2=\frac{\kappa_e^2}{(\kappa_o+\kappa_e)^2+(\omega-\omega_r)^2} \tag{7}$$

When the resonance condition of the cavity is satisfied, i.e.,$\omega=\omega_r$, the transmission spectrum has a dip with a minimal value of $T_{\min}=\kappa_o^2/(\kappa_o+\kappa_e)^2$.

At the resonance frequency, the standing wave modes in the nanoring cavity could be excited. The resonance condition is given by[9]:

$$k_1\frac{J_n(k_1r)}{J_n'(k_1r)}-k_2\frac{H_n^{(1)}(k_2r)}{JH_n^{(1)'}(k_2r)}=0 \tag{8}$$

where $k_1=k_0n_d$ and $k_2=k_0n_m$ are the respective wavevectors in the dielectric disk and in the surrounding metal, and $n_{d,m}$ are the refractive indices of the dielectric and the metal, respectively. J_n is a Bessel function of the first kind and order n, and $H_n^{(1)'}$ is a Hankel function of

the first kind and order n. J_n' and $H_n^{(1)'}$ are the derivatives of the Bessel function and Hankel function, respectively. The first resonance mode (mode 1) is considered in the wavelength range of interest, which corresponds to the first order of the Bessel and Hankel functions.

In this study, the FDTD method with perfectly matched layer absorbing boundary condition is employed to investigate the transmission characteristics of the structure. The nonuniform meshing is applied and the maximal grid size is less than 4 nm for good convergence of the numerical calculations. The TM-polarized incoming pulse is generated at the incident port of the MIM waveguide. The transmitted power flow (defined as $P_x=\int_y (E\times H)x\mathrm{d}y$, which is integrated over the cross section of the waveguide), monitored at the output position of the waveguide, is recorded as a function of time and then Fourier transformed to obtain the corresponding spectral response[10].

Figure 2 shows the transmission spectra of the band-stop filter structure where the width of MIM waveguide w=50 nm and the radius of nanoring cavity R=200 nm. The coupling distance between the waveguide and the cavity is set to t=10, 11, 12, 13, and 15 nm, respectively. Note that the strong evanescent coupling only occurs when the coupling distance t is smaller than the field skin depth in metal (less than 30 nm[11]), which requires high processing precision in the device manufacturing. As shown in Fig.2, there is a small blue shift and growth of the transmission dip as t increases, which can be explained by the temporal coupled-mode theory. The increase of t would result in a smaller coupling strength and a smaller decay rate κ_e, while the κ_o is almost invariant. Consequently, $T_{\min}$ increases with the reduction of κ_e. The bandwidth of the resonance spectra also reduces as t increases, because a large coupling distance can weaken the "cavity" effect.

The resonance wavelengths have nearly linear relations with the cavity radius R when the refractive index is consistent (here n_d=1.7). As a result, the transmission characteristics of the band-stop filter could be manipulated by adjusting the geometrical parameters. The degree of deviation between the center position of the outer disc and the center position of the inner disc is discussed. From Fig.3, we find that this deviation will cause slight drift in the resonant wavelength. We use the control variable method to set the center distance between the inner disk center and the outer disc δ=0, 25, 50, 75 and 100 nm under the geometric parameters of the outer disk R=212 nm, the internal disk r=25 nm, and the gap between waveguide and outer disk t=12 nm.

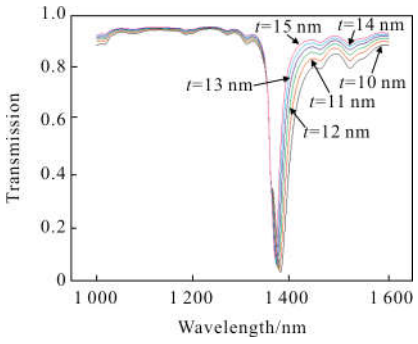

Fig.2 Transmission spectra of the band-stop filter with different coupling distances t when R=200 nm, n_d=1.7, and w= 50 nm

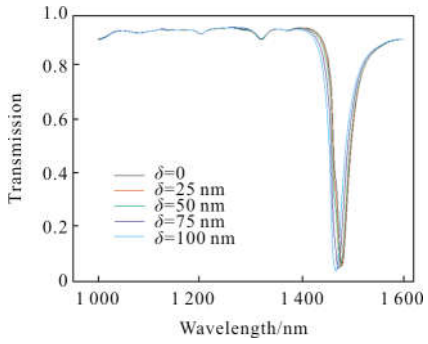

Fig.3 Transmission and the resonant wavelength vary with the distance between the center of the inner disc and the center of the outer disc, δ=0, 25, 50, 75 and 100 nm

We can see from Fig.3 that when the radius of the two discs does not change, the wavelength of the resonant transmission peak will gradually decrease with the increase of the distance between the two disk centers. And we find that the drift of such resonant peak is relatively small, which is about 4 nm each time when the distance is shifted 25 nm. This effect is very conducive to our accurate adjustment of the designed structure.

According to the aforementioned principle, a dual band-stop filter could be obtained by placing two nanoring cavities on the opposite sides of the MIM waveguide. The transmission peaks of two or three combined nanorings which have been optimized at the three wavelength of 1 310 nm, 1 490 nm and 1 550 nm are simultaneously observed. We designed the cavity I of R_1=190.5 nm, r_1=25 nm, δ=0 nm for filtering the wavelength λ_1=1 310 nm, cavity II of R_2= 213 nm, r_2=25 nm, δ=102 nm for λ_1=1 490 nm, and cavity III of R_3= 225, r_3=25 nm, δ=0 nm for λ_3=1 550 nm. The coupling distance between the nanoring cavity and the waveguide of 1310 nm and 1 490 nm is set to t=15 nm, and the coupling distance between the nanoring cavity and the waveguide of the 1 550 nm is set to t=12 nm. Figure 4 illustrates the transmission spectra with two or three transmitted dips by using the combination of nanorings. Through combining any two of the three cavities I, II, and III, the transmission spectra with multi transmitted dips at the designed filtered wavelengths are achieved, as shown in Fig.4 (a) - (c). It can be seen that the transmitted -dip wavelengths are consistent with the superposition of the transmission spectrum of single resonator.

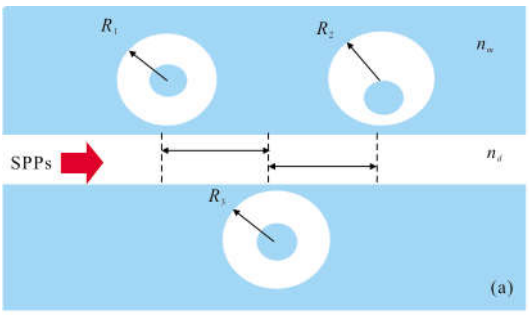

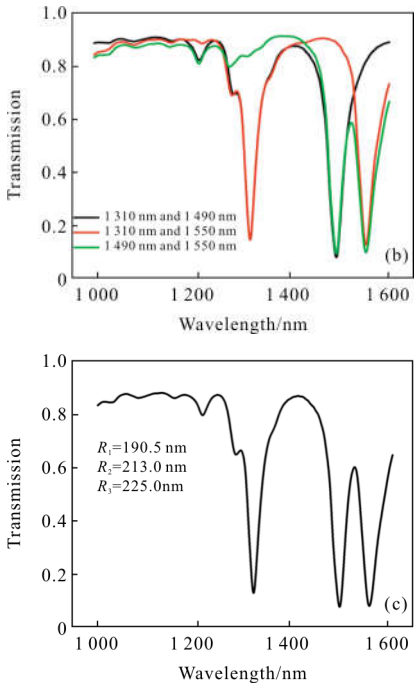

Fig.4 (a) Schematic of a three band-stop filter structure, (b) transmission spectra of the dual band-stop filter with the transmitted-dip wavelengths of 1 310 nm and 1 490 nm, 1 310 nm and 1 550 nm, 1 490 nm and 1 550 nm, (c) the transmission spectra corresponding to three side-coupled nanorings of which dips are at 1 310 nm, 1 490 nm and 1 550 nm

2 Discussion of the triple-wave-length demultiplexing structure

In this section, we employ the dual band-stop plasmonic filters to design a triple-wavelength demultiplexing structure and discuss its performance. Figure 5(a) shows a schematic of the triple-wavelength demultiplexer. The structure consists of three output channels, each of which is sandwiched by two nanoring cavities. The structure parameters are set as w=50 nm, n_d=1.7, R_1=190.5 nm, r_1=25 nm, δ=0 nm for filtering the wavelength λ_1=1310 nm, cavity II of R_2=213 nm, r_2=25 nm, δ=102 nm for λ_2=1 490 nm, and cavity III of R_3=225 nm, r_3=25 nm, δ=0 nm for λ_3=1 550 nm, and L_1=L_2=L_3=L=250 nm. The three

demultiplexed wavelengths are λ_1=1 310 nm, λ_2=1 490 nm, and λ_3=1 550 nm.

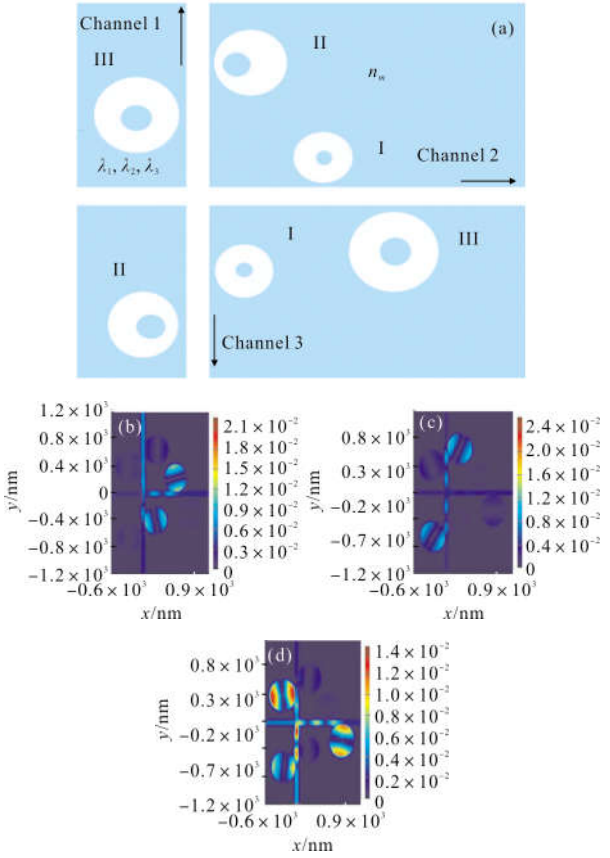

Fig.5 (a) Schematic of a triple-wavelength demultiplexing structure based on dual band-stop filters. (b)-(d) The contour profiles of $|H_z|$ for different incident wavelengths of λ_1=1 310 nm, λ_2=1 490 nm, λ_3=1 550 nm

Each channel filterreturns two undesired wavelengths and transmits the desired one. Transmission spectra of the three channels are depicted in Fig.6. It reveals that the three transmission wavelengths of 1 310 nm, 1 490 nm, and 1 550 nm can be demultiplexed into channels 1-3, respectively. Fig.5 (b)-(d) shows the contour profiles of $|H_z|$ in the structure for the three demultiplexed wavelengths. It is clear that the incident light with the wavelengths of 1 310 nm, 1 490 nm, and 1 550 nm have strong transmission at channel I, II and III, respectively. Moreover, it can be seen that one channel also can be forbidden and return the light at undesired wavelength. Besides, the distances between the edges of the adjacent cavities are set as more than 100 nm, much larger than the field skin depth in metal (less than 30 nm[11]), so that there is no interaction between adjacent cavities.

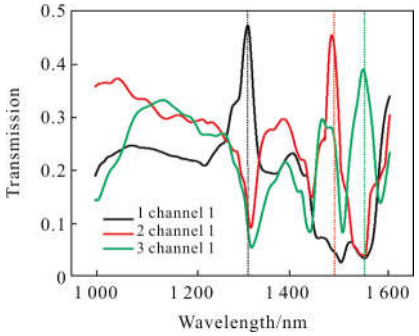

Fig.6 Transmission spectra of three output channels of the proposed structure

As shown in Fig.6, black, red and green solid lines represent the emission spectra from channel 1, channel 2 and channel 3 respectively. The profile of the lines is a little difference, but we can actually see the demultiplexing functions of the three channels in the three communication wavelengths 1 310 nm, 1 490 nm, 1 550 nm. Taking the channel 1 emission spectrum as an example, the channel 1 should transmit 1 310 nm and forbidden 1 490 nm and 1 550 nm, we can see from the black line that the transmission of the 1 310 nm is much higher than that of 1 490 nm and 1 550 nm. Besides, the two undesired wavelengths are seriously suppressed at the meantime. We also can find similar good performance at other two channels.

3 Conclusion

In conclusion, a compact plasmonic triple-wavelength demultiplexing structure based on MIM dual band-stop filters has been proposed and numerically investigated. The operating principle and performance of the device have been analyzed and discussed by using the theoretical model and FDTD simulation. By adjusting the geometric

parameters (i.e., the outer radius and inner radius of the three rings, the coupling gap between the disc and the straight waveguide, the distance between the center of the disc and the center of the outer disc), the demultiplexed wavelength of each output channel could be effectively varied. The proposed structure may find potential applications in highly integrated optical communication systems and nanoscale photonic circuits.

References:

[1] Liu H, Gao Y, Zhu B, et al. A T-shaped high resolution plasmonic demultiplexer based on perturbations of two nanoresonators[J]. ***Opt Commun***, 2015, 334: 164-169.

[2] Neutens P, Dorpe P V, Vlaminck I D, et al. Elec-trical detection of confined gap plasmons in metal-insulator-metal waveg-uides[J]. ***Nat Photon***, 2009, 3: 283-286.

[3] Zhu Zhendong, Bai Benfeng, Tan Qiaofeng. Resonance characteristics of surface plasmon elements on laminated cylindrical table [J]. ***Infrared and Laser Engineering***, 2017, 46(9): 0934001. (in Chinese)

[4] Zhu Mengjun, Zhang Dawei, Chen Jiannong. Design of broadband near-infrared surface plasmon logic and gate devices [J]. ***Infrared and Laser Engineering***, 2016, 45 (3): 0320003.(in Chinese)

[5] Dionne J A, Sweatlock L A, Atwater H A. Plasmon slot waveguides: Towards chip -scale propagation with subwavelength-scale localization[J]. ***Phys Rev B***, 2006, 73: 035407.

[6] Johnson P B, Christy R W. Optical constants of the noble metals[J]. ***Phys Rev B***, 1972, 6: 4370-4379.

[7] Li Q, Wang T, Su Y, et al. Coupled mode theory analysis of mode-splitting in coupled cavity system[J]. ***Opt Exp***, 2010, 18: 8367-8382.

[8] Wang G, Lu H, Liu X, et al. Tunable multi -channel wavelength demultiplexer based on MIM plasmonic nanodisk resonators at telecommunication regime [J]. ***Opt Exp***, 2011, 19: 3513-3518.

[9] Chremmos I. Magnetic field integral equation analysis of interactionbetween a surface plasmon polariton and a circular dielectric cavity embedded in the metal [J]. ***J Opt Soc Amer A***, 2009, 26: 2623-2633.

[10] Hu F, Yi H, Zhou Z. Wavelength demultiplexing structure based on arrayed plasmonic slot cavities [J]. ***Opt Lett***, 2011, 36: 1500-1502.

[11] Huang Lingling. Phase control characteristics and applications of the metamaterials based on chiral light field[J]. ***Infrared and Laser Engineering***, 2016, 45(6): 0634001. (in Chinese)